Eur. J. Biochem. 218, 213–219 (1993)

Structure and dynamics of the acidic compact state of apomyoglobin by frequency-domain fluorometry

Ettore BISMUTO[1], Enrico GRATTON[2], Ivana SIRANGELO[1] and Gaetano IRACE[1]

[1] Dipartimento di Biochimica e Biofisica, Seconda Università di Napoli, Italy
[2] Laboratory for Fluorescence Dynamics, Department of Physics, University of Illinois at Urbana-Champaign, USA

(Received July 1/September 4, 1993) – EJB 93 0983/2

The conformational dynamic properties of tuna apomyoglobin, a single tryptophan-containing protein, in the acidic compact state, as well as in the native and in the fully unfolded state, have been explored by frequency-domain fluorometry. Apomyoglobin at acidic pH in the presence of high salt concentration displays bimodal tryptophanyl lifetime distributions which may be related to the simultaneous presence of different populations of structural states (compact and fully unfolded states). The tryptophanyl anisotropy decay indicated that the acidic compact state displays at least two rotational correlational times, suggesting that this state possesses a complex geometrical organization. 1-Anilino-8-naphthalene sulfonate (ANS), bound both to native and compact protein forms, shows broad unimodal lifetime distributions. The small time dependence of the ANS emission spectra indicated that the solvent dipolar reorganization are either absent or they occur on a time scale much shorter than the lifetime of the excited ANS molecule bound to apomyoglobin. The anisotropy decay data relative to the extrinsic fluorophore (ANS) are consistent with the presence of a single rotational correlation time for both native (12.1 ns) and compact (6.2 ns) states.

There is much experimental evidence that several proteins have two classes of denatured conformations; a fully unfolded state and a relatively compact one which is often referred as the molten-globule state (Ptitsyn, 1987; Kuwajima, 1989; Dill and Shortle, 1991; Chelvanayagam et al. 1992; Cleland et al., 1992; Daggett and Levitt, 1992; Kuroda et al., 1992; Palleros et al., 1992). This term was introduced to emphasize the possible occurrence, in the unfolding pathway of globular proteins, of intermediates characterized by compact native-like secondary structure but unfolded tertiary structure.

The presence of at least one stable intermediate during the denaturant-induced equilibrium unfolding of apomyoglobin is well established. Specifically, it was shown that a marked deviation from a two state transition exists using guanidinium chloride and/or acid to produce unfolding (Colonna et al., 1982,; Bismuto et al., 1983). Some different spectroscopic approaches, such as second-derivative and thermal-absorption spectroscopies, circular dichroism, steady-state fluorescence, etc. were used to deduce the structural characteristics of the intermediate resulting from the denaturant action (Irace et al., 1986, Ragone et al., 1987, Bismuto et al. 1992). Recently, Goto and Fink (1990) constructed a pH/ionic strength phase diagram for apomyoglobin which describes the stability regions for the native, compact and fully unfolded forms.

It has been suggested that a protein in a given conformational state will not remain in a unique conformation but will fluctuate among a large number of conformational substates (for a review see Frauenfelder and Debrunner, 1983). Different substates have the same overall structure but differ in small details (Frauenfelder et al., 1979). The emission decay of intrinsic or extrinsic fluorophores bound to apomyoglobin is dependent on the number of such subconformations as well as on the interconversion rate among these substates. Recent studies demonstrated that the tryptophanyl fluorescence emission of apomyoglobin as well as that of 2,6-*p*-toluidinenaphthalene sulfonate bound to the heme pocket of the apoprotein can be represented by a quasi continuous-lifetime distribution (Bismuto et al., 1988; Bismuto and Irace, 1988; Bismuto et al., 1989a; 1989b). More recently, it was shown that the tryptophanyl fluorescence decays of fully unfolded polypeptides are characterized by broader lifetime distributions whose width at half maximum is logarithmically related to the polypeptide chain length (Bismuto et al., 1991).

The aim of this paper is to explore the conformational dynamic properties of apomyoglobin in the native and denatured structures using the intrinsic tryptophanyl emission decay of tuna apomyoglobin and that of 1,8-anilinonaphthalene sulfonate (ANS) bound to apomyoglobin. Three experimental conditions, differing in ionic strength and pH, were chosen so that apomyoglobin was essentially present as the native, fully unfolded or compact stucture, respectively (Goto and Fink, 1990).

Data were analyzed using continuous-lifetime distributions with the purpose to use the distribution width as an indicator of microheterogeneity. Although the distribution analysis can be substituted with the analysis based on a small number, i.e. three or four exponentially decaying components, both approaches indicate protein microheterogeneity. However, it is difficult to imagine that the acid-unfolded and

Correspondence to E. Bismuto, Dipartimento di Biochimica e Biofisica, 2ª Università di Napoli, Via Costantinopoli, 16, I-80138 Napoli, Italy
Fax: +39 81 5665863.
Abbreviation. ANS, 1-anilino-8-naphthalenesulfonate.

the compact form of the protein adopt only two or three well-defined protein conformations as would be indicated by the discrete exponential analysis. Therefore, we prefer the distribution analysis using the distribution width only as a qualitative parameter that is indicative of protein subconformations. In principle, protein microheterogeneity can be static or dynamic, where the terms refer to a time scale comparable to the lifetime of the excited state. The simultaneous measurement of the anisotropy decay is used to discriminate between the two alternatives.

The results indicate that the compact state of apomyoglobin is a complex globular structure with a large capacity to fast fluctuate among subconformations. In this form of the protein, the amino acid side chains are unable to form stable tertiary interactions among themselves.

MATERIALS AND METHODS

Myoglobin

The main component of tuna myoglobin was prepared according to the method previously described (Bismuto et al., 1989). The homogeneity of the preparations was controlled by sodium dodecyl sulfate/polyacrylamide gel electrophoresis with 15% gels and 5% stacking gels (Laemmli, 1970).

Apomyoglobin

The heme was removed from myoglobin by the 2-butanone extraction procedure (Teale, 1959). The contamination of the apoprotein by myoglobin was assessed spectrophotometrically. In all cases, no significant absorption was observed in the Soret region.

Protein concentration

Myoglobin concentration was determined spectrophotometrically at 407 nm in 0.1 M sodium phosphate, 0.15 M NaCl, pH 7.0, using 139000 M^{-1} cm^{-1} as molar absorption coefficient at 407 nm (Bismuto et al., 1985). For apomyoglobin, the molar absorption coefficient at 280 nm was calculated from the tryptophan and tyrosine content (Colonna et al., 1983) using molar absorption coefficients of 5500 M^{-1} cm^{-1} and 1250 M^{-1} cm^{-1}, respectively (Wetlaufer, 1962).

Chemicals and solutions

All common chemicals were reagent grade and were purchased from British Drug Houses. ANS was a product of Merck Co. and its Mg^{2+} salt was recrystallized twice using the method described by Weber and Young (1964); the ANS concentration was determined using the following molar absorption coefficient at 350 nm: 5×10^3 M^{-1} cm^{-1}.

Time-resolved fluorescence and anisotropy measurements

Frequency-domain techniques were used to measure the fluorescence decay of all samples in the range 2−400 MHz (Gratton et al., 1984). The light source was a high-repetition mode-locked Nd-Yag laser used to pump a rhodamine dye laser yielding a 10-ps pulse output of about 50 mW at 590 nm with a 2-MHz repetition rate. This output was then frequency doubled to 295 nm and its harmonic content was used to excite the sample (Gratton and Limkeman, 1983). The excitation was polarized at the 'magic angle' to eliminate rotational effects on the fluorescence lifetime measurements (O'Connor and Phillips, 1984). The emission was observed using an optical filter combination of UV34 and U340 (from Oriel Corp.) or through a long-wave-pass filter with a cut-off wavelength at 400 nm (Corion LG400F). For time-resolved emission spectra, a set of interference filters from Corion Co. with band widths of 10 nm was used. The temperature was monitored continuously during measurements by attaching a thermocouple to the sample cuvette. The readings of the thermocouple were monitored by an Omega Digicator (from Omega Engineering) with an accuracy of ±0.1 °C. The data analysis of lifetime and anisotropy determinations were performed by Global Unlimited (University of Illinois at Urbana; Beechem and Gratton, (1988)). Time-resolved emission spectra were obtained by collecting multifrequency data at several emission wavelengths. At each emission wavelength, the fit was performed using a sum of exponentials. This was undertaken to generate an analytical function which describes the observed decay. The number of exponentials varied over 2−4, depending on the wavelength. The number of exponentials to be used was determined by increasing the number of components until the chi-square value was not further improved. The reconstructed emission spectrum at the selected times was normalized in order to match to the steady-state spectrum (Bismuto et al., 1987).

RESULTS

Emission decay of intrinsic fluorophore

The phase shifts and demodulation factors of the intrinsic-fluorescence emission of tuna apomyoglobin were collected by exciting at 295 nm using modulation in the frequency range 2−400 MHz. The whole emission band was collected. Three different environmental conditions were selected: 0.01 M sodium phosphate, pH 7.4; 0.013 M HCl, pH 2.5; 0.013 M HCl, 0.2 M NaCl, pH 2.5. Under these conditions, the polypeptide chain is found in the native, fully unfolded and compact forms, respectively (Goto and Fink, 1990).

Table 1 shows the results of the non linear least square fit of the emission decays analyzed as sum of discrete exponential components. Table 2 shows the results obtained analyzing the decay as a quasi continuous-lifetime distribution. The best fits, as judged on the basis of chi-square values, were those corresponding to bimodal-lifetime distributions having lorentzian shape. Fig. 1 shows the lifetime distribution pattern relative to the three states of the protein. The emission decay of apomyoglobin at neutral pH is essentially representable by a single narrow lorentzian distribution (Fig. 1A). The short lifetime component which contributes negligible to the total fluorescence probably originates from weakly scattered light or other unpredictable instrumental contributions (Barbieri et al., 1990). In contrast to the native protein form, the fluorescence decay of acidic apomyoglobin at pH 2.5 in the absence of salt is represented by a broad lifetime distribution, centered at 0.9 ns, with a significant second narrow distribution located at 2.5 ns (Fig. 1C). At least four discrete exponential components are needed to obtain comparable fits, as judged by the chi-square value. We interpret the large increase of distribution width with respect to native apomyoglobin, i.e. over 0.25−2.39 ns, as due to a large extent of protein heterogeneity. This more complex de-

Table 1. Lifetime discrete analysis of tuna apomyoglobin at different pH and ionic strengths.

Tuna apomyoglobin	Lifetime discrete analysis at		
	neutral pH	acidic pH + salt	acidic pH
Monoexponential			
Lifetime	2.50	2.19	1.84
chi-square	60.1	388	593
Biexponential			
lifetime 1	2.69	3.50	2.71
fraction 1	0.97	0.79	0.80
lifetime 2	0.14	0.62	0.54
chi-square	5.09	22.5	12.5
Triexponential			
lifetime 1	24.2	5.33	14.2
fraction 1	0.00	0.39	0.05
lifetime 2	2.68	1.94	2.37
fraction 2	0.97	0.52	0.81
lifetime 3	0.00	0.29	0.43
chi-square	5.60	4.21	3.30

Table 2. Lifetime lorentzian distribution analysis of tuna apomyoglobin at different pH and ionic strengths.

Tuna apomyoglobin	Lifetime lorentzian distribution at		
	neutral pH	acidic pH + salt	acidic pH
Unimodal			
center	2.57	2.26	1.92
width	0.68	2.60	1.68
chi-square	12.4	19.0	13.7
Bimodal			
center 1	2.67	3.05	2.50
width 1	0.23	1.21	0.05
fraction 1	0.97	0.76	0.28
center 2	0.00	0.61	0.88
width 2	0.05	2.11	2.39
chi-square	1.41	2.13	1.93

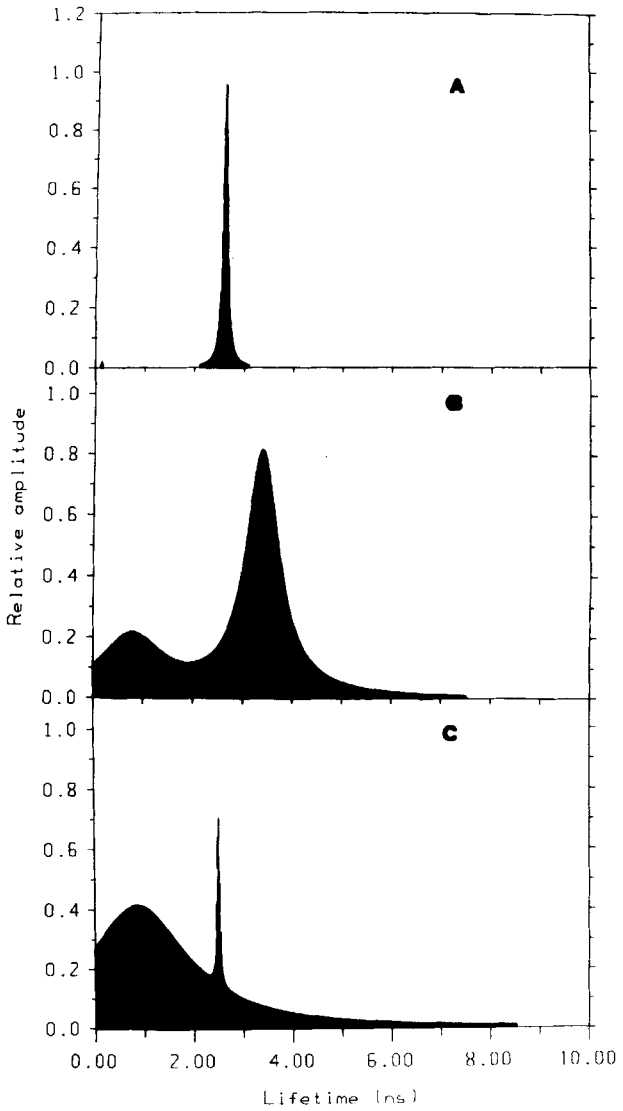

Fig. 1. Tryptophanyl lifetime distribution pattern of different conformational states of apomyoglobin at 20 °C. (A) 0.01 M sodium phosphate, pH 7.4; (B) 0.013 M HCl, 0.2 M NaCl, pH 2.5; (C) 0.013 M HCl, pH 2.5. The excitation wavelength was 295 nm and the emission was observed through a band-pass filter in the range 320–380 nm.

cay is probably generated by fluctuations of the protein matrix in the fully unfolded state (Frauenfelder and Gratton, 1985; Bismuto et al., 1988; Bismuto and Irace,1988). The origin of the second narrow component centered at 2.5 ns might be due to a partial folding by chloride anions added to produce the acidic pH value.

The acidic compact form of apomyoglobin shows an even greater fluorescence heterogeneity (Fig. 1B), which produces two well separated peaks in the lifetime distribution, suggesting the existence of two subpopulations. To examine whether the two peaks in Fig. 1B actually represent physically distinct species each with characteristic internal dynamics, we studied the dependence of the lifetime distribution on the emission wavelength. Fig. 2 shows the tryptophanyl lifetime distribution of the high salt acidic form of apomyoglobin obtained collecting the blue and red side, i.e. at 320 nm and 360 nm, of the emission band. Both distributions are bimodal with similar centers. In contrast, the width of the long-lived component is dramatically reduced at the longest emission wavelength, i.e. 1.1–0.05 ns.

Emission decay of extrinsic fluorophore

ANS, a currently used naphthalene sulfonate probe, is able to form stable non-covalent complexes with both native as well as acidic compact apomyoglobin (Stryer, 1965; Bismuto et al., 1985; Bismuto et al., 1992). In the absence of salt, apomyoglobin at acidic pH is unable to bind ANS molecules, as indicated by the weakly fluorescent signal observed in this condition.

Frequency-domain emission data were performed by exciting the ANS-apomyoglobin complex at 350 nm using a modulation frequency range of 1–200 MHz. The whole emission band was collected through a long-wave-band-pass filter (LG 400). Table 3 summarizes the results of the data analysis. The best fits were obtained using a lorentzian lifetime distribution model; Fig. 3 shows the lorentzian lifetime distributions for the ANS-apomyoglobin complex at pH 7.4 and at pH 2.5 in the presence of 0.2 M NaCl. Both distributions are very broad, the widths being equal to 4.5 ns and

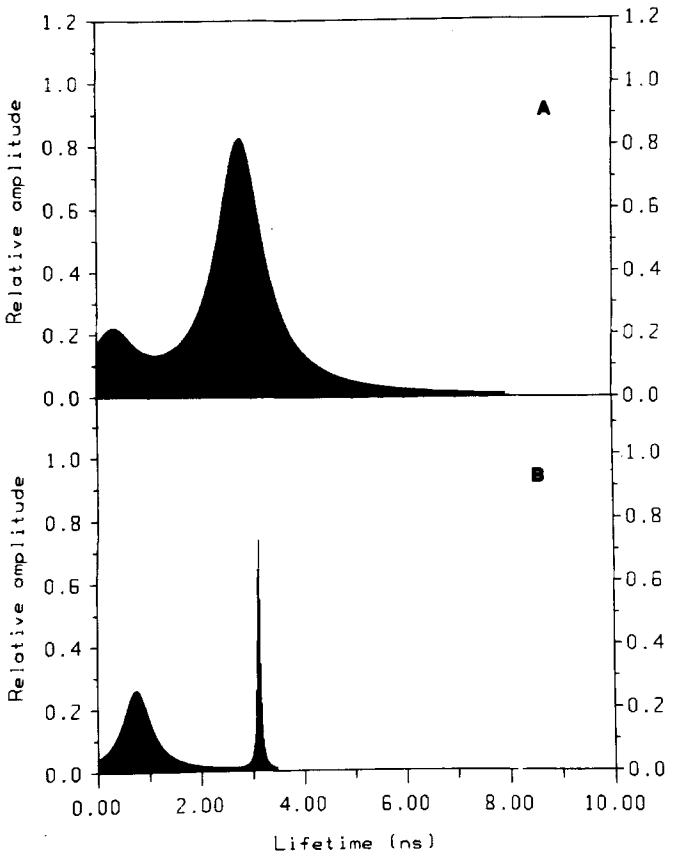

Fig. 2. Tryptophanyl lifetime distribution pattern of apomyoglobin at pH 2.5 in the presence of 0.2 M NaCl. The excitation wavelength was 295 nm and the emission was observed through interferential filter (Corion P-10) at 320 nm (A) and 360 nm (B).

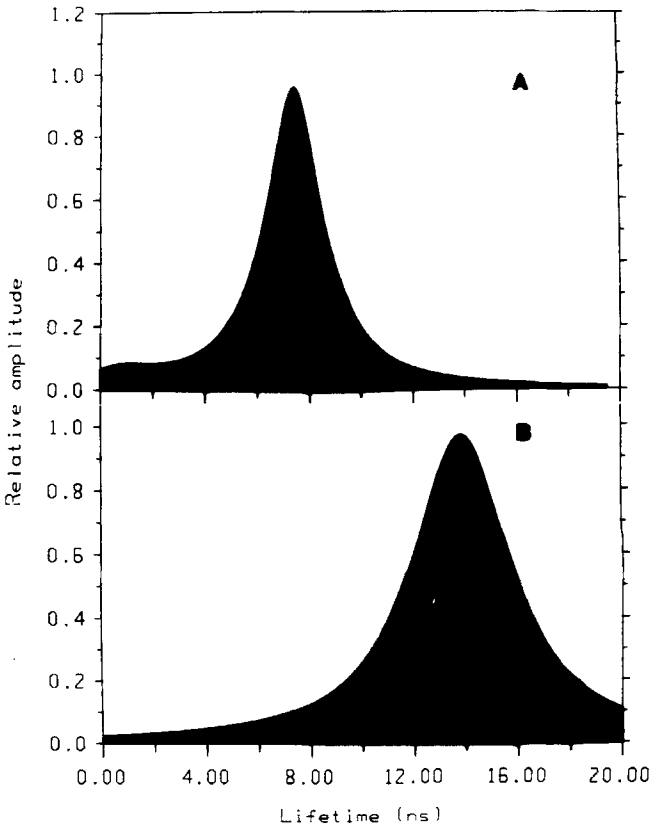

Fig. 3. Lifetime distribution pattern of ANS bound to the native and acidic compact apomyoglobin using bimodal lorentzian distribution at 20°C. (A) 0.013 M HCl, 0.2 M NaCl, pH 2.5; (B) 0.01 M sodium phosphate, pH 7.4. The excitation wavelength was 340 nm and the emission was observed through a LG400 Corion filter. The ANS/apomyoglobin molar ratio was less than 0.2. The chi-square values were 1.21 for (A) and 1.09 for (B).

Table 3. Lifetime analysis of tuna ANS-apomyoglobin at different pH and ionic strengths.

Tuna ANS-apomyoglobin	Lifetime analysis at	
	neutral pH	acidic pH + salt
Monoexponential		
lifetime	11.6	6.7
chi-square	64.8	348
Biexponential		
lifetime 1	14.0	8.0
fraction 1	0.95	0.90
lifetime 2	1.16	1.40
chi-square	31.2	15.4
Unimodal lorentzian distribution		
center	13.6	7.4
width	4.5	2.4
chi-square	1.3	1.03

2.4 ns for ANS bound to native and acidic compact apoprotein, respectively. The distribution centers are also quite different (13.6 ns and 7.4 ns for neutral and acidic proteins, respectively), probably as a consequence of a different solvent accessibility to ANS fluorophore in the two structural states.

Time-resolved emission spectra

The time-resolved emission spectra for ANS-apomyoglobin complexes in the two examined conditions, i.e. at neutral and salt-containing acidic pH, were obtained considering the emission at eight different wavelengths from the blue to the red side of the ANS emission band. Both the neutral and acidic compact proteins exhibit a quite small spectral relaxation (about 4 nm).

Anisotropy decay

The anisotropy decays of the intrinsic fluorescence of apomyoglobin at different pH and ionic-strength conditions were measured by fluorescence differential polarization in the modulation frequency range 2–400 MHz. The data were analyzed using algorithms which consider the decays as arising from emitting species with distributed lifetimes and not from discrete components corresponding to the centers of the bimodal emission-lifetime distribution. Moreover, the following rotational models were considered: a single anisotropy decay, two anisotropy decays for each component of bimodal-lifetime distribution reported in Fig. 1, and two anisotropy decays not associated with the lifetime distribution components (Ludescher et al.,1987; Szmacinski et al., 1987). The first model provided a good fit only in the case of apomyoglobin in its native form as indicated by the chi-square value (0.79), the actual value of the rotational correlation

Table 4. Anisotropy decays of intrinsic fluorescence of apomyoglobin. Φ and r_0 indicate the rotational correlation time and the anisotropy at zero time, respectively; f is the r_0 fraction associated with the rotational correlation time Φ_1. The subscripts a and b refer to the components present in the bimodal tryptophanyl distribution of Fig. 1.

Intrinsic fluorescence species	Anisotropy decay for apomb pH 7.0								
	Φ_{1a}	Φ_{2a}	r_{oa}	f_{1a}	Φ_{1b}	Φ_{2b}	r_{ob}	f_{1b}	chi-square
	ns				ns				
Two associate	6.56	2.30	0.17	0.99	26.5	1.09	0.25	0.03	0.589
Two non associate	6.43	0.13	0.26	0.66	–	–	–	–	0.523
Intrinsic fluorescence species	Anisotropy decay for apomb pH 2.5 (no salt)								
	Φ_{1a}	Φ_{2a}	r_{oa}	f_{1a}	Φ_{1b}	Φ_{2b}	r_{ob}	f_{1b}	chi-square
	ns				ns				
Two associate	6.37	1.38	0.15	0.18	17.16	0.38	0.24	0.18	2.131
Two non associate	9.06	0.54	0.19	0.24	–	–	–	–	2.133
Intrinsic fluorescence species	Anisotropy decay for apomb pH 2.5 (0.2 m NaCl)								
	Φ_{1a}	Φ_{2a}	r_{oa}	f_{1a}	Φ_{1b}	Φ_{2b}	r_{oa}	f_{1b}	chi-square
	ns				ns				
Two associate	14.52	0.22	0.3	0.63	29.89	1.23	0.19	0.77	1.131
Two non associate	17.92	0.42	0.22	0.77	–	–	–	–	1.051

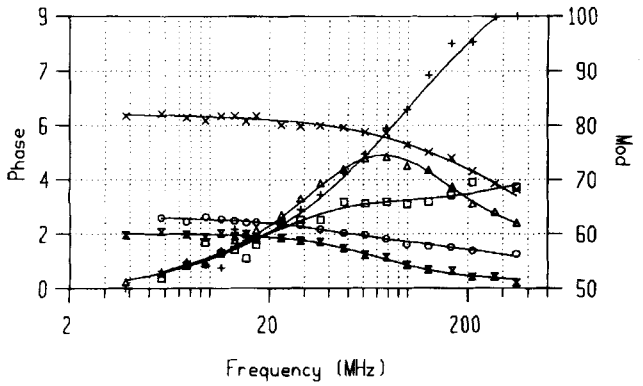

Fig. 4. Frequency-domain anisotropy decays of apomyoglobin with excitation at 295 nm. (△, □, +) Phase shift; ▼, O, X, demodulation factor for neutral, salt-free acidic and salt-containing acidic solutions, respectively. The fits (continuous line), obtained considering associative and non-associative models with two rotational components, were undistinguishable.

time and anisotropy at zero time being 6.23 ns and 0.20, respectively. The anisotropy decay of acidic and salt-containing acidic apoprotein were more complex. Both associative and non associative models well fitted the data. Table 4 summarizes the results. Fig. 4 shows the observed and calculated differential polarization data versus frequency for apomyoglobin in the three examined conditions.

Differential-polarization measurements were performed also for the ANS-apomyoglobin complex at pH 7.4 and at pH 2.5 + 0.2 M NaCl, with excitation at 350 nm. The data fit produced unique rotational correlation times of 12.1 ns and 6.2 ns for native and salt-containing acidic apomyoglobin, respectively (Fig. 5).

DISCUSSION

Acid-denatured apomyoglobin consists of two structural states depending on the pH and salt content; a largely unfolded form and a relatively compact one (Goto et al., 1990; Dill and Shortle, 1991; Bismuto et al., 1992; Murphy et al. 1992). The state-phase diagram of apomyoglobin, constructed on the basis of the observed change in the far ultraviolet circular dichroism, can be correctly predicted by a recently proposed statistical mechanical theory of protein stability (Stigter et al., 1991).

The data reported in this paper indicate that the tryptophanyl emission decay of the acidic compact-state originates from a distribution of fluorescence lifetime. A similar conclusion was also reached for the native and fully unfolded protein. The interpretation of the emission decay of a fluorophore incorporated in a protein matrix in term of continuous-lifetime distribution is a consequence of protein structural fluctuations (Alcalà et al., 1987a; 1987b; Frauenfelder and Gratton, 1985; Frauenfelder et al., 1988). The flexibility of the protein structure generates a great variety of environments that the fluorophore may experience during the excited state. In this respect, the width of the lifetime distribution is an indicator of the number of subconformations that the polypeptide chain can assume and of the interconversion rate among these subconformations. Therefore, the observation that the tryptophanyl lifetime distribution of fully unfolded apomyoglobin is broader than that of the native state is not surprising. The lifetime distribution of the acidic compact state (Fig. 1B) is bimodal with two well separated peaks. A comparison among the data reported in Fig. 1 suggests that the peak centered at a short lifetime (0.9 ns) arises from apomyoglobin molecules that, at pH 2.5 in the presence of 0.2 M NaCl, are still unfolded. The narrow component centered at 2.4 ns, observed in the lifetime distribution pattern of fully

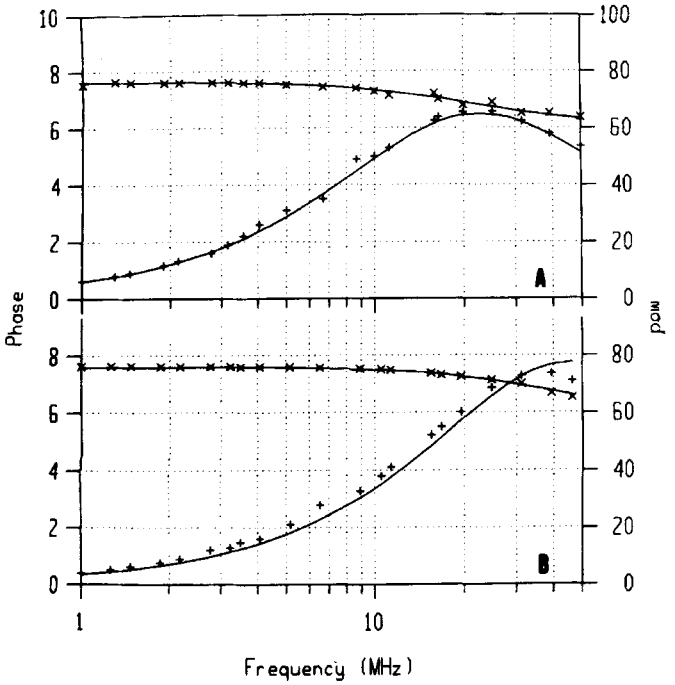

Fig. 5. Frequency-domain anisotropy decays of ANS-apomyoglobin complex with excitation at 340 nm. (+) Phase shift; (×) demodulation factor. The A and B capital letters refer to neutral and salt-containing acidic solutions. The single rotational correlation times obtained by fitting the data (A) and (B) were 12.1 ns and 6.2 ns, respectively.

unfolded apomyoglobin (Fig. 1C), could be related to a small fraction of compact or even native protein molecules. The differences among the distribution centers are probably caused by quenching effects related to different solvent accessibilities to the indolic fluorophore. The broadening of the tryptophanyl lifetime distribution is related to an increased protein microheterogeneity. The origin of protein conformational heterogeneity may be either static or dynamic, where the terms refer to a time scale comparable to the lifetime of the excited state. An attempt to distinguish the nature of the observed fluorescence heterogeneity of the high-salt acidic apomyoglobin was provided by the analysis of the emission decay on the blue and red sides of the emission band. The results indicate that the heterogeneity of the long-lived component in the bimodal-lifetime distribution has a prevalent dynamic character. This is consistent with the high internal flexibility attributed to the molten globule form (Kuwajima, 1989). Circular dichroism spectrum, NMR measurements and proton exchange rate determinations were not able to evidentiate the simultaneous presence of different denatured states of apomyoglobin under similar experimental conditions (Hugson et al., 1990).

The data analysis shown in Table 4 shows that both the associative and non-associative model well describe the anisotropy decays of the compact and fully unfolded state. The shorter correlation rotational times are indicators of the internal tryptophan mobility. It must be pointed out that the associative model, i.e. two anisotropy decays for each component of the bimodal-lifetime distribution, requires a number of free parameters larger than that of the non-associative model, i.e. two anisotropy decays not associated with the lifetime-distribution components. However, the overall picture provided by the associative model appears to be more realistic assuming the co-existence of two different populations of protein states as follows: native, fully unfolded at pH 2.5 in the absence of salt; acidic compact and fully unfolded at pH 2.5 in the presence of 0.2 M NaCl.

Apomyoglobin binds ANS in both neutral and salt-containing acidic solution (Bismuto et al., 1992). The broad lifetime distributions (Fig. 3) indicate that the flexible protein matrix provides a very large number of microenvironments for the extrinsic fluorophore. The reduced width observed for ANS bound to acidic compact apomyoglobin can be due to a higher interconversion rate among conformational substates (Alcalà et al.,1987a; Bismuto et al., 1988). This major flexibility is consistent with the lower value of the distribution center.

The observation that the rotational correlation time of the compact acid form is shorter than that of the native ANS-apomyoglobin complex (12.1 ns and 6.2 ns) suggests that ANS bound to acidic compact apomyoglobin possesses a large mobility.

In conclusion, the behaviour of two distinct apomyoglobin regions in the acidic compact form, i.e., the tryptophan environment and the ANS-binding site, is quite different. In particular, the rotating unit containing the indolic residue displays more complex dynamics than those observed for the apomyoglobin region forming the ANS-binding site. From these studies, we conclude that the compact state behaves as a globular but very flexible structure devoid of a stable tertiary interaction and having an higher solvent accessibility with respect to the native form.

Financial support for this work was provided in part by *Consiglio Nazionale delle Ricerche* (grants 91.02478.CT14 and 92.02263.CT14) and National Institutes of Health (grant RR03155).

REFERENCES

Alcalà, R., Gratton, E. & Prendergast F. (1987a) *Biophys. J. 51*, 587–596.
Alcalà, R., Gratton, E. & Prendergast, F. (1987b) *Biophys. J. 51*, 925–936.
Alonso, D., Dill, K. & Stigter, D. (1991) *Biopolymers* 31, 1631–1649.
Barbieri, B., De Piccoli, F., Gratton, E. (1989) *Rev. Sci. Inst. 60*, 3201–3206.
Beechem, J. M. & Gratton, E. (1988) in *Time-resolved laser spectroscopy in biochemistry* (Lakowicz, J. R., ed.) *SPIE Proceedings 909*, 70–81.
Bismuto, E., Colonna, G. & Irace, G. (1983) *Biochemistry 22*, 4165–4170.
Bismuto, E., Colonna, G., Savy, F. & Irace, G. (1985) *Int. J. Pept. Protein Res. 26*, 195–207.
Bismuto, E., Jameson, D. M. & Gratton, E. (1987) *J. Am. Chem. Soc. 109*, 2354–2357.
Bismuto, E., Gratton, E. & Irace, G. (1988) *Biochemistry 27*, 2132–2136.
Bismuto, E. & Irace, G. (1988) *Photochem. Photobiol. 50*, 165–168.
Bismuto, E., Irace, G. & Gratton, E. (1989a) *Biochemistry 28*, 1508–1512.
Bismuto, E., Sirangelo, I. & Irace, G. (1989b) *Biochemistry 28*, 7542–7545.
Bismuto, E., Sirangelo, I. & Irace, G. (1991) *Arch. Biochem. Biophys. 291*, 38–42.
Bismuto, E., Sirangelo, I. & Irace, G. (1992) *Arch. Biochem. Biophys. 298*, 624–629.
Chelvanayagam, G., Reich, Z., Bringas, R. & Argos, P. (1992) *J. Mol. Biol. 227*, 901–916.
Cleland, J. & Randolph, T. (1992) *J. Biol. Chem. 267*, 3147–3153.

Colonna, G., Balestrieri, C., Bismuto, E., Servillo, L. & Irace, G. (1982) *Biochemistry 21*, 212–215.
Colonna, G., Irace, G., Bismuto, E., Servillo, L. & Balestrieri, C. (1983) *Comp. Biochem. Physiol. 76A*, 481–485.
Daggett, V. & Levitt, M. (1992) *Proc. Natl Acad. Sci. USA 89*, 5142–5146.
Dill, K. A. & Shortle, D. (1991) *Annu. Rev. Biochem. 60*, 795–825.
Frauenfelder, H., Petsko, G. A. & Tsernoglou, D. (1979) *Nature 280*, 558–563.
Frauenfelder, H. & Debrunner, P. (1983) *Annu. Rev. Phys. Chem. 33*, 283–303.
Frauenfelder, H. & Gratton, E. (1985) *Methods Enzymol. 127*, 471–492.
Frauenfelder, H., Parak, F. & Young, R. (1988) *Annu. Rev. Biochim. Biophys. Chem. 17*, 451–479.
Goto, Y. & Fink, A. (1990) *J. Mol. Biol. 214*, 803–805.
Goto, Y., Calciano, L. I. & Fink, A. (1990) *Proc. Natl Acad. Sci. USA 87*, 573–577.
Goto, Y. & Nishikiori, S. (1991) *J. Mol. Biol. 222*, 679–686.
Gratton, E., Jameson, D. M. & Hall, R. (1984) *Annu. Rev. Biophys. Bioeng. 13*, 105–124.
Gratton, E. & Limkeman, M. (1983) *Biophys. J. 44*, 315–324.
Hugson, F. M., Wright, P. E. & Baldwin, R. L. (1990) *Science 249*, 1544–1548.
Irace, G., Bismuto, E., Savy, F. & Colonna, G. (1986) *Arch. Biochem. Biophys. 244*, 459–469.
Kuroda, Y., Kidokoro, S. & Wada, A. (1992) *J. Mol. Biol. 223*, 1139–1153.
Kuwajima, K. (1989) *Protein Struct. Funct. Gener. 6*, 87–103.
Laemmli, U. K. (1970) *Nature 227*, 680.
Lakowicz, J. R., Gratton, E., Laczko, G., Cherek, H. & Limkemann, M. (1984a) *Biophys. J. 46*, 463–477.
Lakowicz, J. R., Gratton, E., Cherek, H., Maliwal, B. P. & Laczko, G. (1984b) *J. Biol. Chem. 259*, 10967–10972.
Ludescher, R. D., Peting, L., Hudson, S. & Hudson, B. (1987) *Biophys. Chem. 28*, 59–75.
Murphy, K. P., Bhakuni, V., Xie, D. & Freize, E. (1992) *J. Mol. Biol. 227*, 293–306.
O'Connor, D. V. & Phillips, D. (1984) *Time-correlated single photon counting*, 1st edn., pp. 257–261, Academic Press, New York.
Palleros, D., Reid, K., McCarty, J., Walker, G. & Fink, A. (1992) *J. Biol. Chem. 267*, 5279–5285.
Ptitsyn, O. B. (1987) *J. Protein Chem. 6*, 272–293.
Ragone, R., Colonna, G., Bismuto, E. & Irace, G. (1987) *Biochemistry 26*, 2130–2134.
Stigter, D., Alonso, D. & Dill, K. A. (1991) *Proc. Natl Acad. Sci. USA 88*, 4176–4180.
Stryer, L. (1965) *J. Mol. Biol. 13*, 482–495.
Szmacinski, H., Jayaweera, R., Cherek, H. & Lakowicz, J. R. (1987) *Biophys. Chem. 27*, 233–241.
Teale, F. W. J. (1960) *Biochem. J. 76*, 381–388.
Wetlaufer, D. B. (1962) *Adv. Protein Chem. 17*, 303–390.
Weber, G. & Young, L. B. (1964) *J. Biol. Chem. 239*, 1415–1423.